THE ASTROPHYSICAL JOURNAL, 468:L85–L89, 1996 September 10

NONCOSMOLOGICAL SIGNAL CONTRIBUTIONS TO THE *COBE*[1] DMR 4 YEAR SKY MAPS

A. J. BANDAY,[2,3,4] K. M. GÓRSKI,[2,5] C. L. BENNETT,[6] G. HINSHAW,[2] A. KOGUT,[2] AND G. F. SMOOT[7]
Received 1996 January 9; accepted 1996 June 28

ABSTRACT

We limit the possible contributions from noncosmological sources to the *COBE* Differential Microwave Radiometer (DMR) 4 year sky maps. The DMR data are cross-correlated with maps of rich clusters, extragalactic *IRAS* sources, *HEAO 1* A-2 X-ray emission, and 5 GHz radio sources using a Fourier space technique. There is no evidence of significant contamination by such sources at an rms level of ~8 μK [95% confidence level (c.l.) at 7° resolution] in the most sensitive 53 GHz sky map. This level is consistent with previous limits set by analysis of earlier DMR data and by simple extrapolations from existing source models. We place a limit on the rms Comptonization parameter averaged over the high-latitude sky of $\delta y < 1 \times 10^{-6}$ (95% c.l.). Extragalactic sources have an insignificant effect on the cosmic microwave background power spectrum parameterizations determined from the DMR data.

Subject headings: cosmic microwave background — diffuse radiation — intergalactic medium

1. INTRODUCTION

In this Letter, we address the potential for contamination of the cosmic microwave background (CMB) anisotropy in the *COBE* DMR 4 year sky maps (Bennett et al. 1996) by astrophysical foregrounds outside of our Galaxy. We investigate possible contributions from noncosmological sources by direct comparison of the DMR sky maps with similar maps generated from extragalactic surveys.

Models of the point-source contribution at the DMR frequencies (Toffolati et al. 1995) suggest a contribution $\Delta T/T < 10^{-7}$, well below the level at which they may be of concern. Simple frequency extrapolations of the *IRAS* point-source fluxes (Gawiser & Smoot 1996) reach the same conclusion. However, such calculations are not sensitive to the more extended diffuse emission that some of the maps considered here may contain.

2. METHOD

At a given frequency, the DMR sky map can be considered a superposition of signal contributions due to true cosmological anisotropy, instrument noise, and other astrophysical sources. In this Letter, we attempt to limit the last of these by specifically cross-correlating the DMR maps with a given extragalactic sky map X over the high-latitude sky.

Inverse noise variance–weighted combinations of the A and B channels in Galactic pixelization are formed at each of the three DMR frequencies, the weights being (0.618, 0.382), (0.579, 0.421), and (0.382, 0.618) at 31.5, 53, and 90 GHz, respectively. Each of the three DMR maps, together with the extragalactic sky map, is decomposed into coefficients ($\boldsymbol{c}_{\rm DMR}$) using a basis of orthonormal functions explicitly computed on the incompletely sampled sky (Górski 1994), a procedure which is directly analogous to the expansion of a full-sky map in terms of spherical harmonic coefficients. The available sky coverage is defined as the region with Galactic latitude above 20° minus additional regions at Ophiuchus and Orion (Banday et al. 1996), hereafter referred to as the custom DMR Galactic cut, and at specific positions with missing data. This technique has the advantage of allowing exact exclusion of the monopole and dipole components from the analysis (which are unimportant for the investigation of cosmological anisotropy), and makes full use of all the available spatial (phase) information. The measured DMR map coefficients in the new orthogonal basis at a given frequency, $\boldsymbol{c}_{\rm DMR}$, can then be written in vector form as $\boldsymbol{c}_{\rm DMR} = \boldsymbol{c}_{\rm CMB} + \boldsymbol{c}_N + \alpha_X \boldsymbol{c}_X$, where $\boldsymbol{c}_{\rm CMB}$, $\boldsymbol{c}_N$, and $\boldsymbol{c}_X$ are the coefficients describing the true CMB distribution, the noise, and the extragalactic map; α_X is now a coupling constant (with units $\mu{\rm K}\,X^{-1}$) to be determined by minimizing

$$\chi^2 = (\boldsymbol{c}_{\rm DMR} - \alpha_X \boldsymbol{c}_X)^T \tilde{\boldsymbol{M}}^{-1} (\boldsymbol{c}_{\rm DMR} - \alpha_X \boldsymbol{c}_X),$$

where $\tilde{\boldsymbol{M}}$ is the covariance matrix describing the correlation between different Fourier modes on the cut sky and is dependent on assumed cosmic microwave background (CMB) model parameters and the DMR instrument noise. Full details of its computation can be found in Górski (1994) and Górski et al. (1996). The CMB may be sufficiently described by a Harrison-Zeldovich power-law spectrum with rms quadrupole normalisation $Q_{\rm rms-PS} \sim 18$ μK (Banday et al. 1996; Górski et al. 1996). The coefficient vectors contain spectral information over a range $[\ell_{\rm min}, \ell_{\rm max}]$, where $\ell_{\rm min}$ is either 2 (quadrupole included) or 3 (quadrupole excluded). We set $\ell_{\rm max} = 30$, which is sufficient to describe the cosmic content of the DMR data.

By minimising the χ^2 with respect to α_X, we find that the coupling constant α_X has an exact solution

$$\alpha_X = \boldsymbol{c}_X \tilde{\boldsymbol{M}}^{-1} \boldsymbol{c}_{\rm DMR} / \boldsymbol{c}_X \tilde{\boldsymbol{M}}^{-1} \boldsymbol{c}_X$$

and a Gaussian error given by $\sigma^2(\alpha_X) = (\boldsymbol{c}_X \tilde{\boldsymbol{M}}^{-1} \boldsymbol{c}_X)^{-1}$.

[1] The National Aeronautics and Space Administration/Goddard Space Flight Center (NASA/GSFC) is responsible for the design, development, and operation of the *Cosmic Background Explorer* (*COBE*). Scientific guidance is provided by the *COBE* Science Working Group. GSFC is also responsible for the development of the analysis software and for the production of the mission data sets.

[2] Hughes STX Corporation, Laboratory for Astronomy and Solar Physics, Code 685, NASA/GSFC, Greenbelt, MD 20771.

[3] Current address: Max-Planck-Institut für Astrophysik, Karl-Schwarzschild-Strasse 1, 85740 Garching bei München, Germany.

[4] banday@mpa-garching.mpg.de.

[5] On leave from Warsaw University Astronomical Observatory, Al. Ujazdowskie 4, PL-00-478 Warszawa, Poland.

[6] Laboratory for Astronomy and Solar Physics, Code 685, NASA/GSFC, Greenbelt, MD 20771.

[7] LBL, SSL, and CfPA, Building 50-25, University of California, Berkeley, CA 94720.

TABLE 1

CROSS-CORRELATION RESULTS AND NONCOSMOLOGICAL SIGNAL CONTRIBUTIONS

FREQUENCY (GHz)	QUADRUPOLE INCLUDED			QUADRUPOLE EXCLUDED			JOINT ANALYSIS		
	α_X (μK X^{-1})	$(\alpha T_X)_{rms}$ (μK)	$(\alpha T_X)_{pp}$ (μK)	α_X (μK X^{-1})	$(\alpha T_X)_{rms}$ (μK)	$(\alpha T_X)_{pp}$ (μK)	α_X (μK X^{-1})	$(\alpha T_X)_{rms}$ (μK)	$(\alpha T_X)_{pp}$ (μK)
ACO Rich Clusters									
31	−10.34 ± 8.74	6.2 ± 5.3	47.9 ± 39.9	−4.60 ± 9.64	2.1 ± 4.4	17.9 ± 37.4	0.37 ± 8.51	0.2 ± 5.0	1.3 ± 30.7
53	1.72 ± 4.78	1.0 ± 2.9	7.8 ± 21.8	2.79 ± 4.97	1.3 ± 2.3	10.8 ± 19.3	5.85 ± 4.52	3.4 ± 2.6	21.1 ± 16.3
90	3.30 ± 6.04	2.0 ± 3.6	15.1 ± 27.5	3.77 ± 6.38	1.7 ± 2.9	14.6 ± 24.8	1.10 ± 5.52	0.6 ± 3.2	4.0 ± 19.9
HEAO 1 A-2 X-Ray Sources									
31	46.60 ± 23.52	7.5 ± 3.8	112.5 ± 56.8	43.71 ± 23.69	6.8 ± 3.7	102.8 ± 55.7	52.87 ± 26.79	7.6 ± 3.8	113.2 ± 57.35
53	28.12 ± 11.09	4.6 ± 1.8	67.9 ± 26.8	27.97 ± 11.10	4.4 ± 1.7	65.8 ± 26.1	4.65 ± 12.14	0.7 ± 1.7	10.0 ± 26.0
90	22.84 ± 14.93	3.7 ± 2.4	55.1 ± 36.0	22.89 ± 14.97	3.6 ± 2.3	53.8 ± 35.2	15.54 ± 16.21	2.5 ± 2.3	37.5 ± 34.7
1.2 Jy *IRAS* Galaxies									
31	0.75 ± 0.42	8.0 ± 4.5	124.1 ± 69.3	0.85 ± 0.42	8.7 ± 4.3	138.8 ± 68.6	0.48 ± 0.37	5.3 ± 4.1	80.3 ± 61.9
53	0.21 ± 0.19	2.3 ± 2.1	35.2 ± 32.4	0.22 ± 0.20	2.3 ± 2.0	36.3 ± 31.7	0.04 ± 0.17	0.5 ± 1.9	7.4 ± 28.3
90	0.01 ± 0.26	0.2 ± 2.8	2.5 ± 43.8	0.02 ± 0.26	0.2 ± 2.7	2.8 ± 42.6	0.27 ± 0.22	3.0 ± 2.4	45.0 ± 37.1
5 GHz (87 GB/PMN) Radio Sources									
31	0.09 ± 0.14	2.9 ± 4.4	69.9 ± 106.8	0.08 ± 0.15	2.5 ± 4.4	60.7 ± 105.7	−0.09 ± 0.15	2.7 ± 4.6	65.4 ± 111.0
53	0.09 ± 0.06	2.6 ± 1.9	62.7 ± 45.9	0.09 ± 0.06	2.6 ± 1.9	62.5 ± 45.3	−0.01 ± 0.06	0.4 ± 1.9	9.4 ± 47.0
90	0.11 ± 0.09	3.4 ± 2.6	81.7 ± 62.9	0.11 ± 0.09	3.4 ± 2.6	81.8 ± 62.1	0.06 ± 0.09	1.7 ± 2.6	40.9 ± 63.0

Note.—rms and peak-peak values are computed after subtraction of the monopole, dipole, and, where appropriate, quadrupole distributions over the uncut regions of the sky. All temperatures are in thermodynamic units.

The contribution of X to the DMR sky is the map $\alpha_X T_X$ (where T_X is in the natural units of the extragalactic sky map so that this scaled quantity is in μK), which can be characterized by the rms amplitude and peak-to-peak quantity $(\alpha_X T_X)_{rms}$ and peak-to-peak quantity $(\alpha_X T_X)_{pp}$. Both values are computed over the cut sky after subtraction of a best-fit monopole, dipole, and, if appropriate, quadrupole.

3. ABELL-CORWIN-OLOWIN RICH CLUSTERS

Inverse Compton scattering of CMB photons from hot intracluster gas causes a decrement in the Rayleigh-Jeans part of the CMB spectrum, $\Delta T = -2yT_0$, where T_0 is the unperturbed CMB temperature and y, the Comptonization parameter, is a function of the integrated electron pressure along the line of sight. As suggested by Hogan (1992), this Sunyaev-Zeldovich (SZ) effect (Sunyaev & Zeldovich 1980) might generate some of the temperature anisotropy observed by *COBE* DMR. As in Bennett et al. (1993), we use a rich cluster map constructed from the data of Abell, Corwin, & Olowin (1989, hereafter ACO) to place limits on this contribution. We therefore assume that the ACO rich cluster map is a good tracer of the spatial morphology of the large-scale cluster gas distribution giving rise to the SZ effect and that the richness class is a good indicator of the optical depth of the gas. Each pixel of the rich cluster map is a sum over the richness classes of all clusters in that pixel. The map is convolved with the DMR beam pattern (Wright et al. 1994b). Additional versions of the map have been computed with different Abell richness class thresholds and by summing over the richness class exponentiated by various powers. No significant differences are seen for the different binning strategies. We report results for a minimum richness class threshold of 1 and a simple binning by the richness class (i.e., an exponent of 1).

Table 1 summarizes the results of the analysis. The SZ effect will generate approximately equal and negative α_X values over the three DMR frequencies. There are no significant correlations between the DMR sky maps and the ACO rich cluster map.

4. *HEAO 1* A-2 X-RAY DATA

The *HEAO 1* A-2 X-ray emission map, as discussed in Bennett et al. (1993) and provided by K. Jahoda with flux scale as in Jahoda & Mushotzky (1989), was reconvolved to the DMR beam profile and cross-correlated with the DMR sky maps. After applying the custom DMR Galactic cut, 3875 pixels remain at high latitude. Strong Galactic emission from the Ophiuchus and Orion regions, common to both the X-ray and DMR maps, is excised by this process. Nevertheless, there remain positive correlations in excess of 2 σ. A significant fraction of the correlation appears to be associated with the LMC—a prominent high-latitude feature in the *HEAO 1* map. The correlation coefficient is recomputed between the 53 GHz map and the X-ray map after removing a circular region of 10° radius centered on the LMC: we find that α_X falls to $\sim 20 \pm 15$. At 95% confidence, we limit the contribution of anisotropy traced by the X-ray map to the DMR analysis to be less than 8 μK, irrespective of its origin.

Since rich clusters of galaxies are bright X-ray sources, in principle, the X-ray emission in the *HEAO 1* map could also trace the hot gases in these structures that give rise to the SZ effect (although the angular distribution of the X-ray emission and temperature anisotropy would be somewhat different). We might then expect some negative correlation with the DMR maps (since, at DMR frequencies, the SZ effect manifests itself as a temperature decrement), but in all cases the correlation constants are positive. We conclude, in agreement

with previous work by Bennett et al. (1993), Boughn & Jahoda (1993), and Rephaeli (1993), that the fluctuations observed by *COBE* are not generated by such a mechanism.

5. 1.2 Jy *IRAS* GALAXIES

We consider a sample of objects selected from the *IRAS* point-source catalog with measured redshifts, in order to specifically select extragalactic sources. Fisher et al. (1995) extend the 2 Jy survey of Strauss et al. (1992) to a flux limit of 1.2 Jy, resulting in a catalog of some 5321 galaxies with measured redshifts covering 87.6% of the sky. As described previously, a map of the 1.2 Jy sky was generated using the *IRAS* 100 μm flux, but excluding regions as prescribed in Strauss et al. (1990), and using a mask and software provided by Strauss (1995). The *IRAS* 100 μm sky is dominated by emission from the LMC, but we are more interested in potentially significant correlations with the rest of the map. The existing mask does exclude a region around the LMC. After applying the mask and the custom DMR Galactic cut, 3620 pixels remain. The *IRAS* galaxies show notable structure around Virgo, Coma, and in the supergalactic plane; however, no correlations with the DMR data exceed $\sim 2\ \sigma$ significance.

6. 5 GHz RADIO SOURCES

We have combined data from the 87 GB 5 GHz survey of Gregory & Condon (1991) with new southern hemisphere data from the Parkes-MIT-NRAO (PMN) surveys. The PMN data are divided into declination ranges as follows: the southern survey covers $-87\overset{\circ}{.}5 < \delta < -37°$ (Wright et al. 1994a), the zenith $-37° < \delta < -29°$ (Tasker et al. 1996), the tropical $-29° < \delta < -9\overset{\circ}{.}5$ (Griffith et al. 1994), and the equatorial $-9\overset{\circ}{.}5 < \delta < +10°$ (Griffith et al. 1995). Together with the 87 GB coverage of $0° < \delta < +75°$, in principle, we should be able to construct a nearly all-sky radio source map. Unfortunately, the various data sets are complete at different flux limits, ranging from ~25 mJy for the 87 GB data and parts of the southern survey to ~72 mJy for the zenith survey (Wright 1995). Two maps were therefore assembled: the first with a lower flux threshold of 40 mJy and *excluding* the zenith survey data, the second with a threshold of 72 mJy and *including* the zenith survey. In both cases, data in the declination range $0° < \delta < 10°$ were taken from the 87 GB survey: although some inconsistencies exist between the 87 GB catalog and the PMN catalog over this common declination band (Gregory et al. 1994), small positional uncertainties are unlikely to be of importance after smoothing to DMR resolution. Large systematic differences in the flux densities would generate a strong gradient between the northern and the southern celestial hemispheres that is not observed in the maps.[8]

Cross-correlation of both maps with the DMR data shows no statistically significant difference in the results, and we have elected to continue the analysis with the 72 mJy flux-limited map, which has the greater sky coverage (~12 sr). Off the Galactic plane, much of the signal appears toward Virgo. After applying the custom DMR Galactic cut to the map, 3690 usable pixels (covering ~7.5 sr) remain. No correlations exceed the $\sim 1\ \sigma$ level.

[8] Furthermore, replacing the PMN southern survey with an alternative version from Gregory et al. (1994) that was generated in a similar fashion to the 87 GB catalog also yields statistically consistent results.

7. JOINT ANALYSIS

Previously, we fitted each extragalactic sky map to each DMR sky map separately. In this section, we extend the template-fitting technique (as fully described in Górski et al. 1996) to enable us to fit the four noncosmological template maps to the three DMR frequencies simultaneously. This forces the CMB distribution (in thermodynamic units) to be invariant between the three frequencies and suppresses the sensitivity of the method to noise features in the individual DMR maps that are clearly not common to all three frequencies. This allows an improved determination of the extent of chance cosmic or noise alignments with the template maps. We include the quadrupole components in the analysis and determine the Galactic contribution by fitting to two Galactic templates—the DIRBE 140 μm map and a radio survey at 408 MHz (Haslam et al. 1981). These two maps are sufficient to trace the Galactic dust, free-free, and synchrotron emission, as discussed in Kogut et al. (1996a, 1996b). Orthonormal functions were computed for the sky coverage common to all template maps, leaving 3423 pixels after the custom DMR Galactic cut was made (the region around the LMC was therefore masked since it is removed in the *IRAS* 1.2 Jy analysis). No constraints were imposed on the spectral dependences of the template maps over the DMR frequencies. Since the method considers the three DMR maps simultaneously, it results in the strongest constraints on noncosmological correlations. Eighteen coefficients were determined, and the 12 non-Galactic coefficients are summarized in column (8) of Table 1. The results are in excellent agreement with the single DMR channel-to-template fits.

Typical uncertainties in α give a 95% confidence level (c.l.) upper limit on the rms contribution traced by the ACO map of less than $\sim 6\ \mu$K for the sensitive 53 and 90 GHz channels. This yields a corresponding 95% c.l. rms limit on the Comptonization parameter averaged over the high-latitude sky of $\delta y = -(\delta T/2T) \simeq 1 \times 10^{-6}$. If we interpret the limits from the *HEAO 1* A-2 correlations similarly (i.e., as limits on SZ-related fluctuations), this limit improves to less than 8.4×10^{-7}. Rephaeli (1993) has independently searched the *HEAO 1* A-2 database to place direct bounds on the properties of hot gas in superclusters of galaxies, placing a limit on the mean Comptonization parameter of a few times 10^{-7}, in excellent agreement with the results here.

In fact, the correlations between the DMR maps and both the ACO clusters and the *HEAO 1* A-2 X-ray map are predominantly positive, in contrast to the expected signature from the SZ effect. Since the sensitivity of our test may be compromised by competing astrophysical emission, the sign of the correlations may be more significant than the statistical errors suggest. Such a signal could be indicative of radio sources embedded in the clusters. Since the cross-correlation between these maps and the 5 GHz radio sources is negligible, this would require that the dominant sources at DMR frequencies have flat spectra and be below the detection threshold at the lower frequency. We place a conservative 95% c.l. upper limit on the rms *emission* from clusters over the high-latitude sky of 10 μK at 31.5 GHz.

After the exclusion of the LMC region from the joint analysis sky coverage, the 2.5 σ correlation between the 53 GHz sky map and the *HEAO 1* A-2 X-ray map is decreased significantly, in agreement with the computations in § 4. Bennett et al. (1993) predict that the LMC, and specifically the giant H II region 30 Doradus, will contribute a signal of order

TABLE 2

FITTED AMPLITUDES TOWARD SUNYAEV-ZELDOVICH CANDIDATE CLUSTERS (μK)

Source	T_{31}	T_{53}	T_{90}	Weighted Mean
Coma	-3 ± 52	4 ± 16	-59 ± 25	-14 ± 13
	-63 ± 53	5 ± 16	20 ± 26	5 ± 13
Virgo	54 ± 59	-21 ± 17	33 ± 26	-2 ± 14
	-35 ± 60	10 ± 17	-33 ± 27	-4 ± 14
Perseus-Pisces	16 ± 67	1 ± 24	3 ± 37	3 ± 19
	-32 ± 69	25 ± 24	4 ± 38	16 ± 19
Hercules	105 ± 51	9 ± 19	-3 ± 30	15 ± 15
	-54 ± 52	13 ± 19	15 ± 31	8 ± 15
Hydra	-12 ± 62	-29 ± 21	9 ± 32	-25 ± 17
	77 ± 64	-18 ± 21	12 ± 33	-3 ± 17

Note.—First line for each source refers to fitted amplitude of weighted-sum map, the second refers to the (A − B)/2 difference map. All amplitudes are thermodynamic temperature units.

50 μK at 53 GHz. Kogut et al. (1994) determined an upper limit of 87 μK (95% c.l.) from the 2 year sky maps with a point-source–fitting technique, in good agreement with this prediction. Using the peak-peak limits from the earlier fits that included this region, we place 95% upper limits to the antenna temperature microwave emission of the LMC of 109, 49, and 57 μK at 31.5, 53, and 90 GHz, respectively.

In addition, the correlation coefficients between the Galactic templates and the 4 year maps are in good agreement with those determined in Kogut et al. (1996b). For comparison, at 53 GHz, we find $\alpha_{140\ \mu m} = 2.45 \pm 1.04$, $\alpha_{408\ MHz} = 0.36 \pm 0.76$ to convert the Galactic templates to antenna temperature in μK. There is no significant cross talk between the Galactic and the extragalactic templates.

Finally, we have tested the sensitivity of the fits to the assumption that the cosmic signal present in the DMR sky maps is well described by a power-law spectrum with $Q_{rms-PS} \sim 18$ μK and $n = 1$ by running a full grid of power-law models as in Górski et al. (1996). We compute an average of the α-coefficients weighted by the likelihood function over the grid and find it to be in excellent agreement with those values computed with the Harrison-Zeldovich model. Moreover, we find that the effect of the noncosmological template subtraction on the most likely (Q_{rms-PS}, n) is to shift these values by $\sim$0.1 μK and -0.06, respectively. We conclude that there is no evidence for significant noncosmological signal contamination of the DMR sky maps.

8. CORRELATION WITH INDIVIDUAL BRIGHT CLUSTERS

In the previous sections, we have demonstrated that there is no evidence of noncosmological signal detection based on correlation of the DMR maps with fixed source signal templates. This limit applies to the spatial average of sources at high Galactic latitudes, and so we consider here whether individual bright clusters of galaxies are detected in the DMR data. Nearby clusters are more likely to contribute a measurable signal in the DMR sky maps given their large angular extent. We consider the mean temperatures in the DMR maps toward five nearby clusters, to search for indications of SZ decrements or radio and dust emission from galaxies within the cluster (which are competing effects at the DMR frequencies and any limits should be considered in light of this). A "ring" technique, as utilized previously in Bennett et al. (1993) and Kogut et al. (1994), computes the difference between the mean temperature of pixels within a disk of radius θ and those in the surrounding annulus of equal area. This technique should be sensitive to low surface brightness Comptonization. The results summarized in Table 2 are for $\theta = 10°$. There are no significant detections when a weighted mean is taken over by the three DMR frequencies. The maximum error on this weighted mean (from Table 2) allows us to place a 95% upper limit of 38 μK on emission from nearby clusters.

It is not surprising that the DMR is unable to detect SZ anisotropy from clusters given the large beam dilution. For example, Herbig et al. (1995) have detected the SZ effect in the Coma cluster with a central decrement of -505 ± 92 μK (after large corrections for discrete radio sources and after applying a model for the X-ray atmosphere of the cluster). However, the Coma cluster has an approximate 0°.5 FWHM, which, by virtue of its ratio to the DMR beam solid angle, implies an expected signal of less than 3 μK. A limit of $\delta y < 7 \times 10^{-6}$ can be established for Comptonization by nearby clusters (from the maximum weighted error in Table 2).

9. DISCUSSION AND CONCLUSIONS

We have examined the *COBE* DMR 4 year sky maps for evidence of noncosmological signal contamination and find none. A simultaneous fit of the three DMR frequencies to two Galactic templates and four extragalactic sky maps yields rms limits due to the extragalactic correlations alone of $\sim$18, 8, and 11 μK at 31.5, 53, and 90 GHz, respectively (95% c.l.). These limits are higher than those predicted by simple point-source models, but they are essentially noise-limited estimates (they are in the same ratio as the DMR rms noise levels at each frequency) and must be regarded as somewhat conservative. The contribution from noncosmological sources is insubstantial compared with the $\sim$35 μK rms anisotropy signal detected in the DMR sky maps at 7° resolution (Banday et al. 1996) and, if subtracted in quadrature, would modify the rms amplitude by a small fraction of the noise error. Moreover, the extragalactic template corrections perturb the maximum likelihood power spectrum analysis of the *COBE* DMR data for power-law cosmological models insignificantly: the best-fit parameters (Q_{rms-PS}, n) are only shifted by $\sim$0.1 μK and -0.06, respectively from their uncorrected values.

We acknowledge the efforts of those contributing to the *COBE* DMR. *COBE* was supported by the Office of Space Sciences of NASA Headquarters. We thank Charley Lineweaver and Luis Tenorio for useful comments.

REFERENCES

Abell, G. O., Corwin, H. G., & Olowin, R. P. 1989, ApJS, 70, 1 (ACO)
Banday, A. J., Górski, K. M., Bennett, C. L., Hinshaw, G., Kogut, A., Lineweaver, C., Smoot, G. F., & Tenorio, L. 1996, ApJ, submitted
Bennett, C. L., Hinshaw, G., Banday, A., Kogut, A., Wright, E. L., Loewenstein, K., & Cheng, E. S. 1993, ApJ, 414, L77
Bennett, C. L., et al. 1996, ApJ, 464, L1
Boughn, S. P., & Jahoda, K. 1993, ApJ, 412, L1
Fisher, K. B., Huchra, J. P., Strauss, M. A., Davis, M., Yahil, A., & Schlegel, D. 1995, ApJS, 100, 69
Gawiser, E., & Smoot, G. F. 1996, ApJ, submitted
Górski, K. M. 1994, ApJ, 430, L85
Górski, K. M., Banday, A. J., Bennett, C. L., Hinshaw, G., Kogut, A., Smoot, G. F., & Wright, E. L. 1996, ApJ, 464, L11
Gregory, P. C., & Condon, J. J. 1991, ApJS, 75, 1011
Gregory, P. C., Vavasour, J. D., Scott, W. K., & Condon, J. J. 1994, ApJS, 90, 173
Griffith, M. R., Wright, A. E., Burke, B. F., & Ekers, R. D. 1994, ApJS, 90, 179
———. 1995, ApJS, 97, 347
Haslam, C. G. T., Klein, U., Salter, C. J., Stoffel, H., Wilson, W. E., Cleary, M. N., Cooke, D. J., & Thomasson, P. 1981, A&A, 100, 209
Herbig, T., Lawrence, C. R., Readhead, A. C. S., & Gulkis, S. 1995, ApJ, 449, L5
Hogan, C., 1992, ApJ, 398, L77
Jahoda, K., & Mushotzky, R. F. 1989, ApJ, 346, 638
Kogut, A., Banday, A. J., Bennett, C. L., Górski, K. M., Hinshaw, G., & Reach, W. 1996a, ApJ, 460, 1
Kogut, A., Banday, A. J., Bennett, C. L., Górski, K. M., Hinshaw, G., Smoot, G. F., & Wright, E. L. 1996b, ApJ, 464, L5
Kogut, A., Banday, A. J., Bennett, C. L., Hinshaw, G., Loewenstein, K., Lubin, P., Smoot, G. F., & Wright, E. L. 1994, ApJ, 433, 435
Rephaeli, Y. 1993, ApJ, 418, 1
Strauss, M. 1995, NASA ADS supplement
Strauss, M., Davis, M., Yahil, A., & Huchra, J. P. 1990, ApJ, 361, 49
Strauss, M., Huchra, J. P., Davis, M., Yahil, A., Fisher, K. B., & Tonry, J. 1992, ApJS, 83, 29
Sunyaev, R. A., & Zeldovich, Ya. B. 1980, ARA&A, 18, 537
Tasker, N., Wright, A. E., Griffith, M. R., & Condon, J. J. 1996, AJ, in press
Toffolatti, L., et al. 1995, Astrophys. Lett. Commun., in press
Wright, A. E. 1995, private communication
Wright, A. E., Griffith, M. R., Burke, B. F., & Ekers, R. D. 1994a, ApJS, 91, 111
Wright, E. L., Bennett, C. L., Górski, K. M., Hinshaw, G., & Smoot, G. F. 1996, ApJ, 464, L21

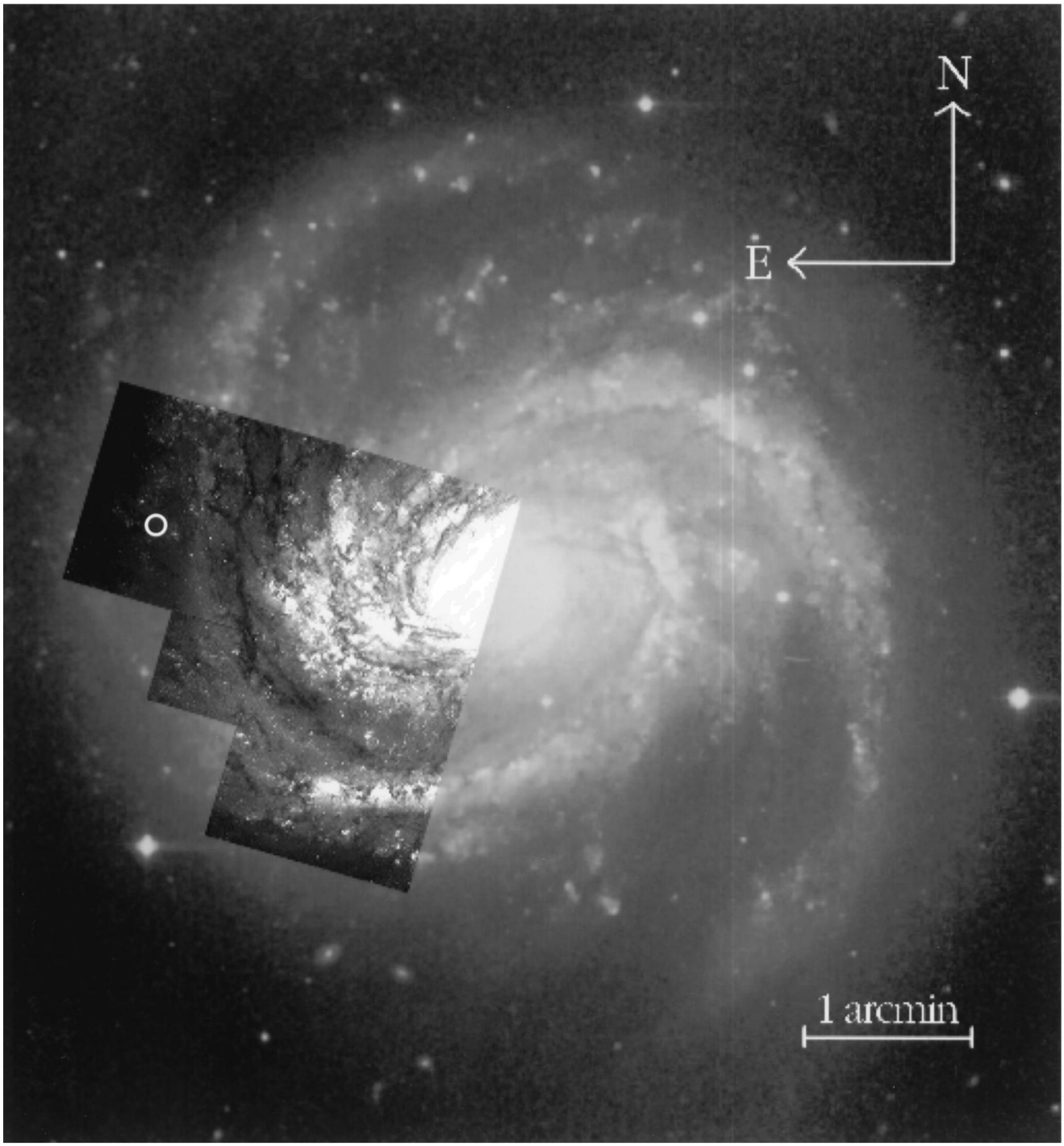

FIG. 1.—Deep *HST*/WFPC2 exposure of M100 superimposed on a ground-based image obtained by R. Peletier with the INT at La Palma. The position of the nova is shown by the white circle.

FERRARESE et al. (468, L96)